The stress state in two-layer hollow cylindrical bars

N. Partaukas*, J. Bareišis**

*Kaunas University of Technology, S.Daukanto 12, 35212 Panėvėžys, Lithuania, E-mail: n.partaukas@gmail.com
**Kaunas University of Technology, S.Daukanto 12, 35212 Panėvėžys, Lithuania, E-mail: jonas.bareisis@ktu.lt

1. Introduction

Multilayer structures (MS) were launched for technical applications in 19th century, but a wider usage was found only in 20th century. Today they are replacing many of the traditional one-material structures. MS has many unique features, but their main advantages are the greater resistance to deformation (e.g. reinforced concrete, steel-coated concrete columns) and qualitatively new physical or chemical characteristics. Materials, their alignment and geometry of the selection options in MS are abundant. Therefore, often, their properties, especially elastic, are not exploited to the maximum. One reason is that the analytical techniques that could facilitate the solution of the issue are in general, either still not created, or they are based on assumptions which are untrue in the structures used.

Variously deforming multilayered structures of different properties, they obtain a complex stress and strain state [1-8]. One of the reasons is the contact pressure arising between the layers of distortion at the time. Its value determines the values of stress components. In the paper [1] the main reason for the contact pressure is radial stretcher on different dimensions, and the axial tightness equals zero. Various structures, particularly pipelines are widely used to reinforce tubes [2-4]. Recently, in the construction industry concrete filled columns have become the commonplace [5, 6, 9, 10]. The specific characteristics of such bars are that they can be exploited even after micro cracks in the core begin.

Research is often limited to stress-state analysis with FEM [2], or analyses are carried out experimentally determining the nature of fracture, strength, strain [3, 5, 9, 10], or such aspects as stability [6]. In case of concrete-filled columns, such a model is acceptable, because to determine analytically stresses of the beginning of micro cracking in the core material is complicated. However, these columns are just one of many possible options for the MS.

A cylindrical rod can be manufactured from several different metals, plastics, or their combinations exposed to elastic deformations. In this case, in order to assess the strength and/or the stiffness it is necessary to know the stress-state components. FEM has been successfully used in the assessment of strength and determination of stress. However, it is difficult to use when it is necessary to determine how the design parameters affect the stress values, under what conditions and why they are increasing, decreasing or becoming extreme values. In addition, FEM results have certain amount of methodological and calculation errors, to determine which it is not easy.

The experimental method for these purposes is even less efficient, as its measurement errors are typically higher than FEM, they are more expensive and time consuming. In our view, the more rational use of two-layer (and other MS) stress analysis is to comprise and analyze the stress analytical expressions, identify typical cases, comparing them with the results of FEM, and only then to determine experimentally the stresses.

The absence of analytical equations and/or FEM model, the complex planning of experiments, selection of suitable equipment and ensuring the reliability of results becomes complicated.

The paper [11] presents the equations of the axial stress for the two-layer bar. They were obtained considering the fact that between the layers there is no axial or radial stretcher, and the Poisson's ratios of the materials are the same. There is no a contact pressure on the seam, and the stress state is axial. The composite rods are manufactured of different materials; therefore the Poisson's ratios are not necessarily the same.

The influence of these ratios for the analytical expressions of stress components in two-layer bars (TB) was estimated in the paper [12]. It has been received that in this case, the stress-state layers are tri-axial. But it has not been answered what value of relative pressure, compared to the axial stress, what it depends upon and how it changes; also what kind of evolution is to the stress state while changing the design parameters, e.g. their dimensions, materials and their arrangement. There is no established methodology and application range. These aspects are important because the methodologies [11] and [12] are fundamentally different in their complexity. When the number of layers is 3 or more, an accurate technique becomes even more complicated than the one presented in the paper [12].

The aim of the paper is to analyze the stress state of two-layer hollow bars, to present the analytical expressions of relative stress in the contact area and to determine the patterns of these variations, depending on cross-sectional area, modules of elasticity, Poisson's ratios, the layers of geometry and layout.

2. Methodology

The subject matter is the two-layer, thick-wall, axially loaded rod (Fig. 1). Let us consider that the rod does not have its axial and radial tightness. The temperature is constant, or it has no influence upon tightness. When Poisson's ratios of the layers are different, due to different radial and hoop strains of the layers (Fig. 2) a contact pressure between the layers occurs (Fig. 1, pressure not shown).

In this case, in the contact zone the layers are in the tri-axial (spatial) stress state. In addition to the axial stress the stresses in radial and hoop directions emerge. The likelihood that the stress state is tri-axial depends on the ratios of the stress components. If the ring and radial stress is infinitely small, in comparison with the axial, the stress state is close to the axial one.

Then the two-layer bar stresses and strength condition set according to the technique [11] will be close to the real stresses and strength. However, if the hoop and/or radial stresses form a large part of the axial stress, the stress-state is tri-axial or biaxial, and stress value and strength is determined by the methodology [12].

Let us examine a two-layer bar (Fig. 1). Before the initial deformation, the length of the layers (L_1, L_2) is the same and known. The cylinders loaded with axial force, so that their

length and the deformation are equal. Therefore, the axial deformations also have to be equal

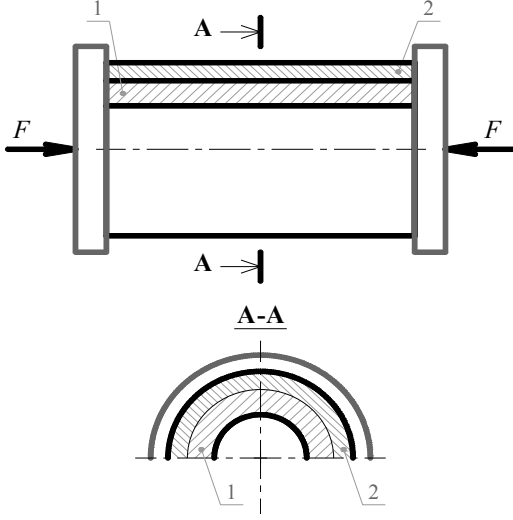$$\varepsilon_{z,1} = \varepsilon_{z,2} \tag{1}$$

Fig. 1 The two-layer hollow rod effected by external force and its cross-section

When the stress state is tri-axial, according to Hooke's Law, axial strains of the layers are as follows

$$\varepsilon_{z,i} = \frac{\sigma_{z,i} - \nu_i \left(\sigma_{r,i} + \sigma_{\theta,i} \right)}{E_i} \tag{2}$$

Having written the Eq. (1) in stress obtain the following

$$\frac{\sigma_{z,1} - \nu_1 \left(\sigma_{r,1}\{\rho\} + \sigma_{\theta,1}\{\rho\} \right)}{E_1} =$$
$$= \frac{\sigma_{z,2} - \nu_2 \left(\sigma_{r,2}\{\rho\} + \sigma_{\theta,2}\{\rho\} \right)}{E_2} \tag{3}$$

where $\sigma_{r,i}\{\rho\}$ and $\sigma_{\theta,i}\{\rho\}$ are radial and hoop stress in the layers, with the radial coordinate ρ.

From Lame equations it is known that the sum of radial and circumferential stresses is independent of the radius. Since axial stresses are independent on the radius, the Eq. (3) is true with any radius ρ. If we consider that the construction is not subjected to external and internal pressures then

$$\frac{\sigma_{z,1} + p_c \, 2\nu_1 \phi_1}{E_1} = \frac{\sigma_{z,2} - p_c \, 2\nu_2 \varphi_2}{E_2} \tag{4}$$

where p_c is contact pressure between the layers; $\varphi_i = \frac{r_i^2}{R_i^2 - r_i^2}$, $\phi_i = \frac{R_i^2}{R_i^2 - r_i^2} = \varphi_i + 1$; r_i, R_i are the inner and outer radius of the layer respectively.

In Eq. (4) there are three unknowns: $\sigma_{z,1}$, $\sigma_{z,2}$ and p_c. Therefore there must be two additional equations. The second is obtained from the static equilibrium, considering that axial stresses in cross-section are distributed uniformly:

$$F = \pi \sigma_{z,1} \left(R_1^2 - r_1^2 \right) + \pi \sigma_{z,2} \left(R_2^2 - r_2^2 \right) \tag{5}$$
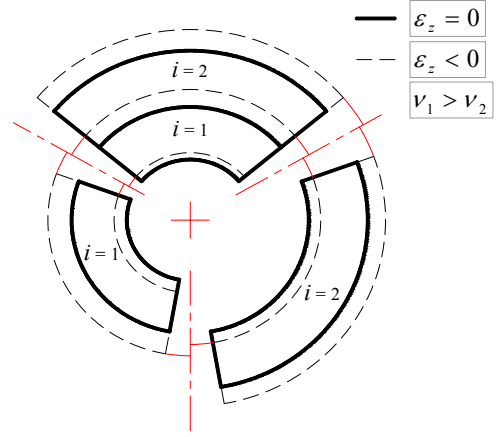

Fig. 2 The internal ($i = 1$), external ($i = 2$) layers, two-layer bar elements and their lateral strain

The third equation is obtained assuming that the contact after deformation persists, (the layers remain bonded). When in the initial moment the radial tightness between the layers equals zero ($R_1 = r_2$), then after deformation

$$\Delta r_2 = \Delta R_1 \tag{6}$$

where Δr_2 is the dimension change of the outer layer inner radius; ΔR_1 is the dimension change of the inner layer outer radius.

In case the layer delaminates, then the contact pressure disappears and the stress turns to axial state. In such cases the axial stresses are calculated according to methodology [11].

In paper [12] it was proved that radial strains of the cylinder are in direct proportion to hoop, therefore

$$\Delta \rho = \rho \varepsilon_{\theta}\{\rho\} \tag{7}$$

where ρ, $\Delta\rho$ is the radius and its change; $\varepsilon_{\theta}\{\rho\}$ is hoop strain, with radial coordinate ρ.

Using Eq. (7) and taking into account that radial tightness between the layers equals zero, the equation (6) may be written as

$$\varepsilon_{\theta,2}\{r_2\} = \varepsilon_{\theta,1}\{R_1\} \tag{8}$$

Having transformed strains to the stresses we obtain

$$\frac{\sigma_{\theta,2}\{r_2\} - \nu_2 \left[\sigma_{r,2}\{r_2\} + \sigma_{z,2} \right]}{E_2} =$$
$$= \frac{\sigma_{\theta,1}\{R_1\} - \nu_1 \left[\sigma_{r,1}\{R_1\} + \sigma_{z,1} \right]}{E_1} \tag{9}$$

Having applied Lame equations from Eq. (9) we obtain

$$\frac{p_c \left(\phi_2 + \varphi_2 \right) - \nu_2 \left(\sigma_{z,2} - p_c \right)}{E_2} =$$
$$= \frac{-p_c \left(\phi_1 + \varphi_1 \right) - \nu_1 \left(\sigma_{z,1} - p_c \right)}{E_1} \tag{10}$$

In designing a bar it is preferred not to use radial di-

mension of the layers r_i, R_i, but the general cross-sectional area A, the hole radius r and the ratios of the layers cross-sectional area $\psi_{i,j} = A_i/A_j$, $\psi_i = A_i/A$. We shall use these parameters as the principal ones.

Finally from the Eqs. (4), (5), (10) the analytical expressions of axial stress, contact pressure, radial, and hoop stress were obtained

$$p_c = \frac{F\xi_{2,1}\psi_2\psi_1(\nu_1 - \nu_2)}{2\pi r^2\alpha_1 + A\psi_1\beta_1} \tag{11}$$

$$\sigma_{z,1} = \frac{F}{A}\frac{2\pi r^2\alpha_2 + A\psi_1\beta_2}{2\pi r^2\alpha_1 + A\psi_1\beta_1} \tag{12}$$

$$\sigma_{r,1}^c = -p_c \tag{13}$$

$$\sigma_{\theta,1}^c = \sigma_{r,1}^c\left(1 + \frac{2\pi r^2}{A\psi_1}\right) \tag{14}$$

$$\sigma_{z,2} = \frac{F\xi_{2,1}}{A}\frac{2\pi r^2\alpha_3 + A\psi_1\beta_3}{2\pi r^2\alpha_1 + A\psi_1\beta_1} \tag{15}$$

$$\sigma_{r,2}^c = \sigma_{r,1}^c \tag{16}$$

$$\sigma_{\theta,2}^c = -\sigma_{r,2}^c\left(\frac{2\pi r^2}{A\psi_2} + \frac{1+\psi_1}{\psi_2}\right) \tag{17}$$

where

$$\alpha_1 = \left(\xi_{2,1}\psi_2(\nu_1 - 1) + \psi_1(\nu_2 - 1)\right)\times$$
$$\times\left(\xi_{2,1}\psi_2(\nu_1 + 1) + \psi_1(\nu_2 + 1)\right)$$

$$\beta_1 = 2\psi_1^2(\nu_2^2 - 1) - \psi_1\psi_2\left(\nu_1 + 1 + \xi_{2,1}(3 - \nu_1 - 4\nu_1\nu_2)\right) -$$
$$- \xi_{2,1}\psi_2^2\left(\nu_2 + 1 - \xi_{2,1}(2\nu_1^2 + \nu_1 - 1)\right)$$

$$\alpha_2 = \xi_{2,1}\psi_2(\nu_1\nu_2 - 1) + \psi_1(\nu_2^2 - 1)$$

$$\beta_2 = 2\psi_1(\nu_2^2 - 1) + \psi_2\left(\xi_{2,1}(2\nu_1\nu_2 + \nu_1 - 1) - \nu_2 - 1\right)$$

$$\alpha_3 = \psi_2\left(\xi_{2,1}(\nu_1^2 - 1) + 1\right) + \psi_1\nu_1\nu_2 - 1$$

$$\beta_3 = 2(\nu_1\nu_2 - 1) + \psi_2\left[1 - \left(\xi_{2,1} + (2\nu_1 + 1)(\nu_2 - \xi_{21}\nu_1)\right)\right]$$

$\sigma_{i,j}^c$ is the stress state component in contact zone of the layers ($i = z$, r or θ); $\xi_{i,j} = E_i/E_j$.

These Eqs. (11)-(17), and their detailed deduction, using other notations, is presented in [12].

In order to determine the stress state (axial, biaxial or tri-axial) it is not only important to know the numerical values of stress state components, but also their ratios, i.e. how big the contact pressure or hoop and radial stress in comparison with axial stress is. The stress state in the material will depend on these ratios.

If the radial and hoop stresses are very small in comparison with the axial ones, then the stress in the layer will be close to the axial one. In contrast, when the radial and hoop stresses represent a noticeable part of the axial stress, the stress state becomes spatial, so therefore, the application of formulas [11] to calculate the axial stress may not correspond the real tension and the bar strength.

To assess the stress state in the layer relative stresses will be used

$$\vartheta_{r,i}^c = \frac{\sigma_{r,i}^c}{\sigma_{z,i}} \tag{18}$$

$$\vartheta_{\theta,i}^c = \frac{\sigma_{\theta,i}^c}{\sigma_{z,i}} \tag{19}$$

where $\vartheta_{r,i}^c$, $\vartheta_{\theta,i}^c$ are relative radial (r), and hoop (θ) stress of the i-layer in the contact zone (c) respectively.

3. Results

Using Eqs. (18), (19) let us analyze how the stresses change when relative dimensions, materials and their arrangement are changed.

The most generic case is the hollow rod ($r>0$), then, after putting expressions (11)-(17) into the Eqs. (18), (19), we obtain

$$\vartheta_{r,1}^c = \frac{A\xi_{2,1}\psi_1\psi_2(\nu_2 - \nu_1)}{2\pi r^2\alpha_2 + A\psi_1\beta_2} \tag{20}$$

$$\vartheta_{\theta,1}^c = \frac{\xi_{2,1}\psi_2(\nu_2 - \nu_1)(A\psi_1 + 2\pi r^2)}{2\pi r^2\alpha_2 + A\psi_1\beta_2} \tag{21}$$

$$\vartheta_{r,2}^c = \frac{A\psi_1\psi_2(\nu_2 - \nu_1)}{2\pi r^2\alpha_3 + A\psi_1\beta_3} \tag{22}$$

$$\vartheta_{\theta,2}^c = \frac{\psi_1(\nu_1 - \nu_2)(2\pi r^2 + A(1+\psi_1))}{2\pi r^2\alpha_3 + A\psi_1\beta_3} \tag{23}$$

When the cross-sectional area of the bar is constant, from the numerical value of the inner radius it will depend whether the layers are thin-walled or thick-walled. Eqs. (20)-(23) show that the relative stresses depends on the cross-sectional area A and the radius r.

From the condition of thin-walled cylinders $2r/(R-r) > 20$, we obtain that the bar and its layers will be thin-walled, when

$$r > \frac{10\sqrt{A}}{\sqrt{21\pi}} \approx 1.231\sqrt{A} \tag{24}$$

When $0 < r < 1.231\sqrt{A}$, the layers can be thin-walled or thick-walled. It depends on the inner radius r, and the ratios of cross-sectional areas of the layers: ψ_1, ψ_2.

The inner layer is thin-walled, when

$$0 < \psi_1 < \frac{21\pi}{100}\frac{r^2}{A} \approx 0.660\frac{r^2}{A} \tag{25}$$

Accordingly, the outer layer is thin-walled when

$$0 < \psi_2 < \frac{21(A + \pi r^2)}{121A} \approx 0.174 - 0.026\frac{r^2}{A} \tag{26}$$

The Eqs. (20)-(26) demonstrate that changing the di-

mensions n times, the stress and cross-sectional relatios will not change (the ring radius changes n times, its cross-sectional area changes as n^2).

Thus the stress ratios are independent of scale. Therefore, the stress ratios in one construction will be equal to the stress ratios in another, if the cross-sections of the construction are proportional and materials and mechanical characteristics are identical. In order to analyze the stress ratios, the inner radius and cross-sectional area can be chosen freely.

Let us analyze the bar, in which: $A = 1.0\,m^2$. Then, the whole bar will be a thin-walled one, when $r \geq 1.231\,m$. Three general cases are possible: a solid bar, a thick-walled or a thin-walled hollow bar (tube). In each case the thickness will depend on the ratios ψ_1 and ψ_2.

To analyze the axial loaded thin-walled tube localized buckling needs to be taken into account, therefore, as it has already been mentioned, we are going to examine the hollow thick-walled construction, choosing the inner radius: $r = 0.5\,m$.

From the Eq. (26), the outer layer is thin-walled when $\psi_2 < 0.31$. The inner layer is thin-walled when $\psi_1 < 0.165$.

As, we analyze the influence of Poisson's ratio; the constructions into the positive and negative ones will be categorized in accordance with the values of their coefficients. The positive construction (PC) is the one in which the axial and radial stress signs are the same, but in the negative one (NC) these signs are opposite.

The PC will be when: $v_1 > v_2$, and the NC when $v_1 < v_2$. Changing the arrangement, the NC or PC-type structure could be obtained. The parameters of the PC and NC variations are pesented in Figs. 3, 4 and 5.

The Poisson's ratios of less rigid materials are generally higher; therefore we consider that the material with the lower elasticity module has a higher Poisson's ratio.

Fig. 3 presents the data showing how the ratios of radial and hoop stresses depend on the inner layer of the relative cross-sectional area (ψ_1). The Poisson's ratios of the layer materials: $v_1 = 0.4$, $v_2 = 0.3$, the elastic module ratios for the PC bar $\xi_{2,1} = 10$, and the NC $\xi_{2,1} = 0.1$, the radial dimension: $r = 0.500\,m$, $R = 0.754\,m$.

In Fig. 3, a we see that when, $\psi_1 = 0$ or $\psi_1 = 1$ the radial stress ratios is zero, since bar composed of one material. So there is no contact pressure, and the relative stresses equal zero.

When $\psi_1 \in (0\ \ 1)$, then the bar is composed of two materials, and since $v_1 \neq v_2$ the contact pressure p_c appears. Because of its impact length of the layers has varied. Since after deformation the layers length should remain the same, there is an increase or decrease in axial stresses. In this case, axial stresses of the exchange ratio of areas (ψ_1), is changing slightly, because the nature of most stress ($\mathcal{G}_{r,i}^c$) affects the contact pressure variation.

The contact pressure appears due to the different layers of transverse strain. Its value does not only depend on the difference of deformation, but also the layers resistance to deformation.

The growth ratio ψ_1 between 0 and 1 of the inner layer of the radial resistance is increasing, while the outer one is decreasing. The value of the contact pressure determines the resistance of the smaller layer.
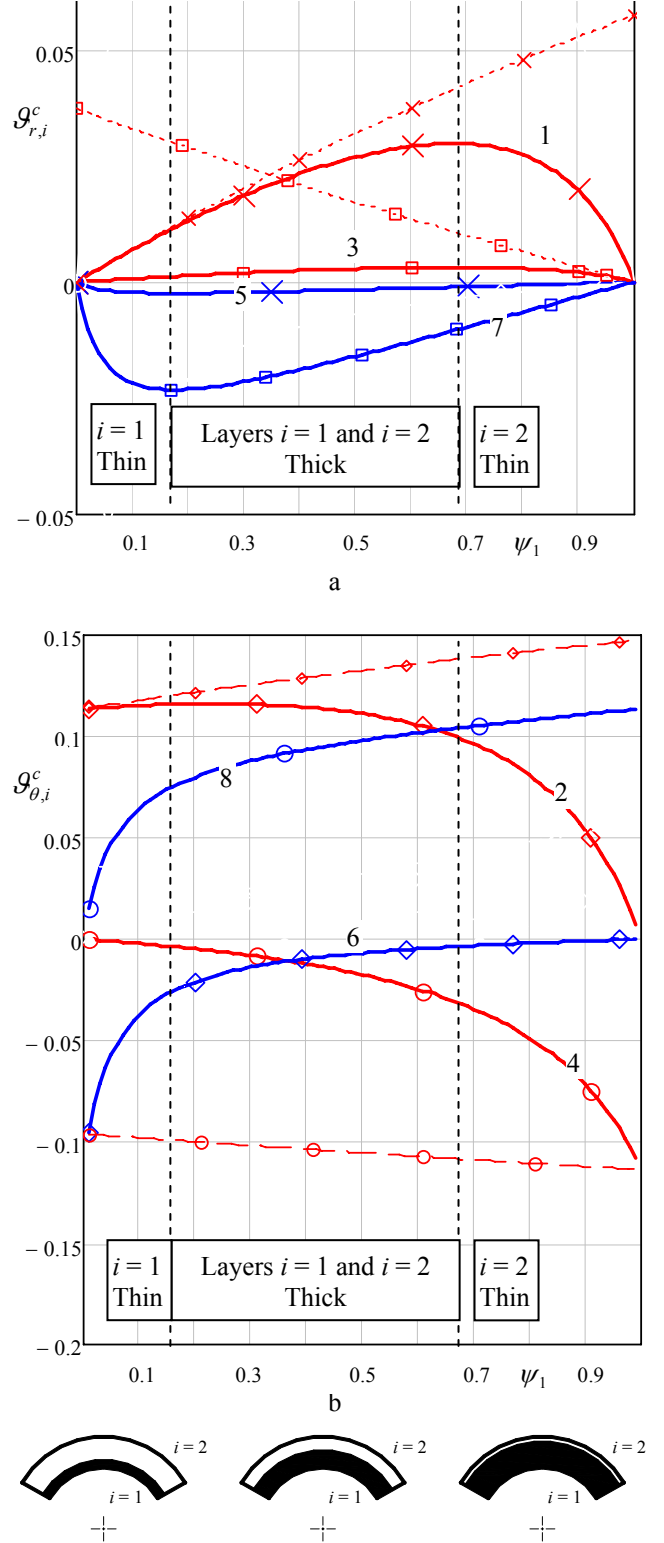

a

b

Fig. 3 The relative radial (a) and hoop (b) variation of the stress-dependence on the inner layer of relative cross-sectional area ψ_1: PC: *1* (-×-) $\mathcal{G}_{r,1}^c$, *2* (- -) $\mathcal{G}_{\theta,1}^c$, *3* (-□-) $\mathcal{G}_{r,2}^c$ and *4* (-○-) $\mathcal{G}_{\theta,2}^c$; NC: *5* (-×-) $\mathcal{G}_{\theta,1}^c$, *6* (-□-) $\mathcal{G}_{\theta,1}^c$, *7* (- -) $\mathcal{G}_{r,2}^c$ and *8* (-○-) $\mathcal{G}_{\theta,2}^c$

Therefore, while the inner resistance is lower, it determines the contact pressure, and p_c and $\mathcal{G}_{r,1}^c$ increase (Fig. 3, a, curve *1*). When resistance of the inner layer is higher than the resistance of the second layer, the contact pressure depends on

the inner layer of resistance.

As it falls, ψ_1 further increases, thus p_c and $\vartheta_{r,1}^c$ begin declining. The relative radial stress $\left(\vartheta_{r,1}^c\right)$ is found in the peak position $\psi_1^{(1)}$ of the Eq. (27)

$$\psi_1^{(1)} = -\frac{\pi r^2 \xi_{2,1} k_6}{\pi r^2 \left(v_2 k_3 + k_2\right) + A k_1} - \frac{\sqrt{\pi r^2 \xi_{2,1} k_6 k_1 \left(\pi r^2 + A\right)}}{\pi r^2 \left(v_2 k_3 + k_2\right) + A k_1} \qquad (27)$$

where $k_1 = v_2^2 - 1$, $k_2 = \xi_{2,1} - 1$, $k_3 = v_2 - \xi_{2,1} v_1$, $k_6 = v_1 v_2 - 1$.

The argument $\psi_1^{(1)}$ largely depends on the ratios of elastic modules $\xi_{2,1}$. When it rises and $\psi_1^{(1)}$ rises as well, the maximum moves from the left to the right and the curve *1* (Fig. 3, a) approaches the curve indicating the limit values of the relative radial stress ($\vartheta_{r,1}^c$) (dotted line Fig. 3, a), the equation of which is as follows

$$f^{(1)}(\psi_1) = \frac{A \psi_1 (v_2 - v_1)}{A \psi_1 \left(v_1(1+v_2) + k_6\right) + 2\pi r^2 k_6} \qquad (28)$$

Using a limit curve (28), it is usually possible to determine the maximum possible relative radial stress available for the construction of the bar. When the quantity πr^2 is sufficiently large in comparison with A, the limit curve turns into a line.

As the axial stresses in stiffer materials are higher, the radial stress ratio value of the outer layer is lower (Fig. 3, a, curve *3*). The nature of the variation is similar to the inner layer (Fig. 3, a, curve *1*), and the value is about 10 times lower due to the same amount of larger axial stresses.

The maximum coordinate of curve *3* (Fig. 3, a) is found from the equality

$$\psi_1^{(2)} = -\frac{\pi r^2 \xi_{2,1} k_5}{\pi r^2 \left(v_1 k_3 + k_2\right) + A k_6} - \frac{\sqrt{\pi r^2 \xi_{2,1} k_5 k_6 \left(\pi r^2 + A\right)}}{\pi r^2 \left(v_1 k_3 + k_2\right) + A k_6} \qquad (29)$$

where $k_5 = v_1^2 - 1$.

The equation of the relative stress $\vartheta_{r,2}^c$, limit curve

$$f^{(2)} = \frac{A(1 - \psi_1)(v_2 - v_1)}{2 A k_6 + 2\pi r^2 k_6} \qquad (30)$$

It should be noted that the maximums of curves *1* and *3* (Fig. 3, a), are generally at different points. The radial and axial stresses in the NC, independently on the axial force, have different signs, so ratio $\vartheta_{r,i}^c$ is negative.

As the NC is obtained from the PC, so the character of stress representing curves *5*, *7* (Fig. 3, a) can be obtained from curves *1*, *3* having put them upside down on the axis $o\psi_1$, and rotated around line $\psi_1 = 0.5$, and switched the indexes.

It should be noted that following the restructuring of curves *1*, *3* we do not receive the real stress values, only their character. This is because the cylinder resistances for the external and internal directions of radial strain are slightly different. The stress values and the maximum limit curves are obtained having applied the Eqs. (27)-(30) for the PC bars, after inserting the NC bar properties into them.

From the Eq. (14) it is obtained that the hoop stresses in the contact zone in their absolute value are not lower than the radial ones

$$\vartheta_{\theta,1}^c \geq \vartheta_{r,1}^c \qquad (31)$$

This results in the geometric characteristics of the layers. When the bar is getting thinner all over the wall or the inner layer, the stress difference increase, and in the solid bar, they become equal.

Relative hoop stress variation in the bar layers $\vartheta_{\theta,1}^c$ and $\vartheta_{\theta,2}^c$ depending on the inner layer of relative cross-sectional area (ψ_1) is presented in Fig. 3, b. It demonstrates that the relative hoop stresses do not necessarily move closer to the zero values, as the ratio ψ_1 moves to the extreme values (i.e. 0 and 1). The reason for this is that even a low pressure can cause a finite amount of hoop stresses in the infinitely small thickness wall.

Therefore, as the ratio ψ_1 goes to the ends of its variation interval, the layer which is currently of infinitely small thickness, reaches finite unequal to zero relative hoop stresses, even if the contact pressure, compared with the axial stresses, is very low (Fig. 3, b, curves *2*, *4*).

While ψ_1 is growing, the inner relative hoop stress (Fig. 3, curve *2*) is initially slightly increasing (at the same time as contact pressure is increasing), and then due to the thinner outer layer wall a rapid decline takes place.

For the same reason, in the outer layer (Fig. 3, b, curve *4*), the relative hoop stresses initially vary slightly, but when ψ_1 gets closer to 1 a rapid increase takes place.

When the contact pressure constitutes a significant part of the axial stress, the relative variation of the hoop stress is determined by both the layers geometry and the contact pressure variation; in case the pressure is small, it is mainly due to the change of geometry.

It has been obtained that changing the ratio of the layer cross sections, the difference between stress $\vartheta_{\theta,1}^c$ and $\vartheta_{\theta,2}^c$ values tends to remain almost constant. By changing the relative thickness of the layers in one layer the relative hoop stress is decreasing while the other is increasing. The relative hoop stress (Fig. 3, b, curve *2*) peak position

$$\psi_1^{(2)} = \frac{\pi r^2 \left(k_3 + k_4\right)}{\pi r^2 k_3 - A k_4} + \frac{r\sqrt{A\left(\pi r^2 + A\right)\pi k_4 \left(2\pi r^2 k_3 - A(k_4 - k_3)\right)}}{A\pi r^2 k_3 - A^2 k_4} \qquad (32)$$

where $k_4 = v_2 - 1$.

The limit curve equations (for curves *2*, *4*)

$$f^{(2)}(\psi_1) = \frac{\left(2\pi r^2 + A\psi_1\right)\left(\nu_2 - \nu_1\right)}{A\psi_1\left(\nu_1(1+\nu_2) + k_6\right) + 2\pi r^2 k_6} \qquad (33)$$

$$f^{(4)}(\psi_1) = -\frac{\left(A(1+\psi_1) + 2\pi r^2\right)\left(\nu_2 - \nu_1\right)}{2Ak_6 + 2\pi r^2 k_6} \qquad (34)$$

Numerical value of the relative hoop stress of the NC-type structure, as well as the relative radial stress event, will be slightly smaller than the PC.

In the previous papers [11-13] a significant influence of material layer elastic modules on the behaviour of multilayer structures was determined. Therefore, it is important to determine the variation in the relative radial and hoop stresses, changing the ratio of elastic modules.

When the construction of the size and value of Poisson's ratios are the same as previously, and the cross-sectional areas of the layers are equal ($\psi_1 = \psi_2 = 0.5$), their stress variations are presented in Fig. 4.

It has been obtained that increasing the ratios of the layer material elastic modules $\xi_{2,1}$, the relative radial stresses of the inner layer of PC increase from zero to the maximum value, but in the outside layer they decrease (curves *1*, *3* Fig. 4, a).

This is due to the axial stress level, which in a stiffer layer is larger, therefore the relative radial stresses are small, and in a less rigid one are high. Having compared the relative radial stress levels of the PC (Fig. 4, a curves *1*, *3*) and NC (curves *5*, *7*) we have obtained that a greater stress is in the layer of a less rigid material with a greater value of Poisson's ratio.

The relative radial strain curves *1*, *3* and *5*, *7*, mainly due to the geometric factor are asymmetrical to line $\xi_{2,1} = 1$.

When the layer is very thin, then the abovementioned curves are symmetrical, and their value is infinitely small. Therefore, in the thin-walled cylinder the radial stress can be ignored. However, the hoop stresses are not equal to zero, so in the thin-walled layer the stress state will be biaxial.

The relative hoop stresses (Fig. 4, b) vary similarly to the radial ones (Fig. 4, a), only differing in their signs and values. The relative hoop stresses in their absolute size will always exceed the relative radial stresses. That difference will be the greater as the wall goes thinner.

The data presented in Fig. 4 demonstrate that both the relative radial and hoop stresses of the PC are higher than the NC, if only the modules of elasticity ratio in the PC are much higher than one. If $\xi_{2,1} << 1$, the relative radial and hoop stresses will be higher in the NC-type bars. This means that having produced the inner layer of less-rigid material it will have higher relative radial and axial stresses than in case this layer is on the outside of the bar.

It should be noted that tensing the PC and compressing the NC the contact zone is tensioned so that if the adhesion between the layers is poor, they can delaminate.

This is an important factor in long-term cyclic test MC, because the resulting gap accelerates the degradation process, reducing the layers of resistance to local buckling.

When $\xi_{2,1} \approx 1$, the relative stress values can change dramatically, but the maximum stress absolute value of both cases is similar. The highest stress is the hoop one.

In this case, until $\xi_{2,1} > 2$, the maximum is always received in the same material (in which ν is greater), despite
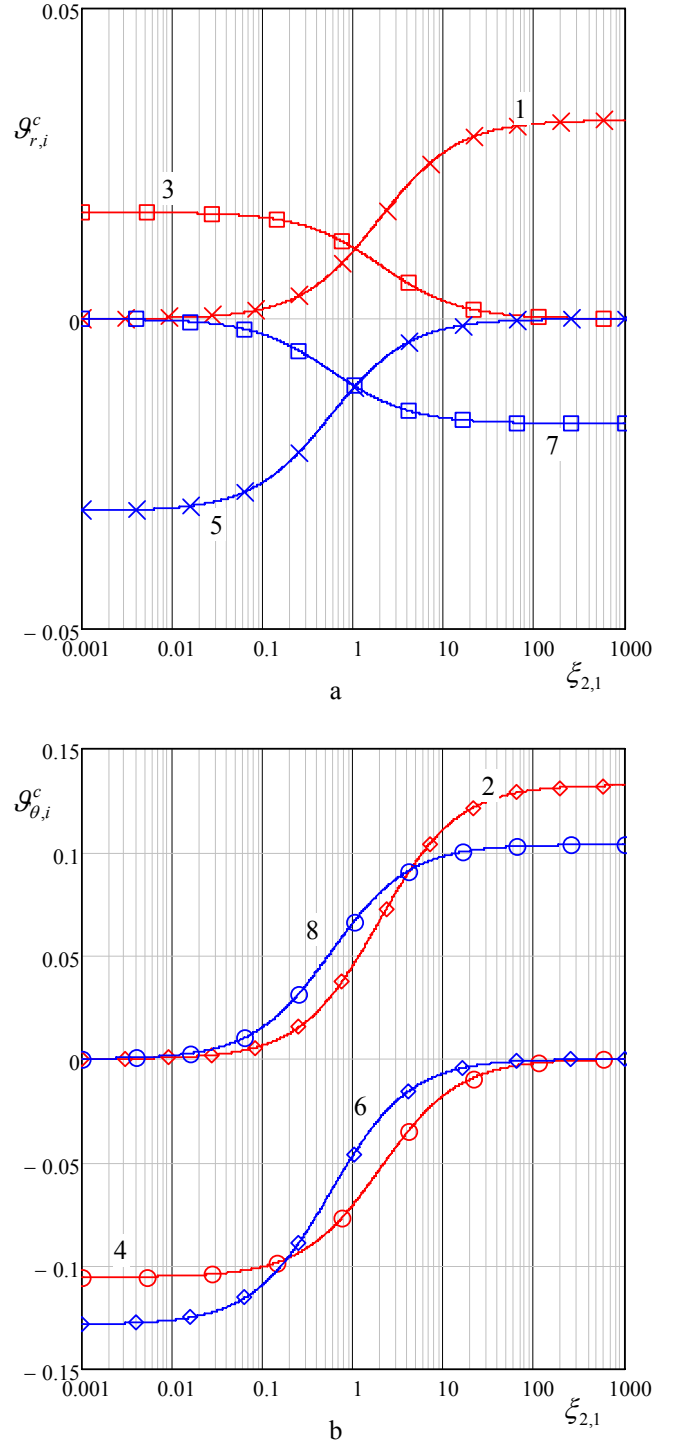

Fig. 4 Variation the relative radial (a) and hoop (b) stress, in hollow construction, depending on elastic modules ratio $\xi_{2,1}$, when $\psi_1 = \psi_2$: PC: *1* (-×-) $\vartheta_{r,1}^c$, *2* (- -) $\vartheta_{\theta,1}^c$, *3* (-□-) $\vartheta_{r,2}^c$, *4* (-○-) $\vartheta_{\theta,2}^c$, NC: *5* (-×-) $\vartheta_{r,1}^c$, *6* (- -) $\vartheta_{\theta,1}^c$, *7* (-□-) $\vartheta_{r,2}^c$, *8* (-○-) $\vartheta_{\theta,2}^c$

the arrangement of materials.

The influence of Poisson's ratios on the relative radial and hoop stress values (Fig. 5) was analysed in the construction of the same dimensions as before, only the outer layer material Poisson's ratio was varied from 0.1 to 0.5, while $\nu_1 = const = 0.3$.

We can see that the stresses are changing linearly and they increase with the Poisson's ratios difference between the layers of the bar.
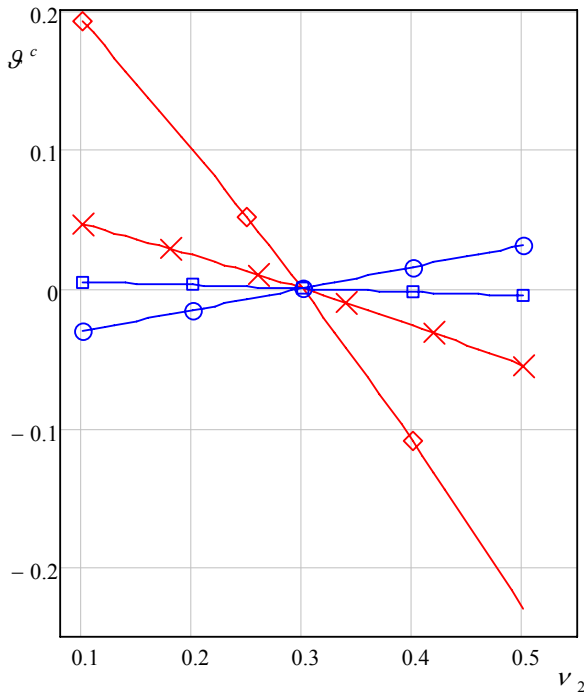

Fig. 5 Stress ratios: (-×-) $\vartheta_{r,1}^c$, (- -) $\vartheta_{\theta,1}^c$, (- □-) $\vartheta_{r,2}^c$, (-○-) $\vartheta_{\theta,2}^c$ dependences on ν_2 values, when $\psi_1 = \psi_2$, and $\xi_{2,1} = 10$

It should be noted that numerical values of the relative radial stress $\left(\vartheta_{r,1}^c\right)$ in the inner layer were the highest.

The outer layer of the relative radial and circular stresses is smaller as a result of higher axial stress values.

When the difference of Poisson's ratio between the layers is equal to zero, the stress state is linear. All curves intersects at the one point (Fig. 5), and the stress ratios are equal to zero.

The relative stress values do not only depend on Poisson's ratios difference, but they also depend on their numerical values.

The closer the Poisson's ratio is to 0.5, the higher are the relative stresses at the same difference between the ratios.

4. Conclusions

A mathematical model for the two-layer axially loaded cylindrical bars stresses state components (axial, radial and hoop) and their limit value determination was presented.

To determine the stress state in the layer analytical expressions (20)-(23) of the relative stress in the contact zone, were obtained. These expressions enable the assessment of the available construction; a stress state is triaxial, biaxial or axial.

Extreme boundaries of relative stress to determine the limit curve and its equation were proposed.

It was obtained that the relative stresses depend on the following factors.

1. Poisson's ratios values. The more they differ the greater the contact pressure and relative radial and hoop stresses are. Moreover, when Poisson's ratio of the material is closer to 0.5, the relative stresses are higher, although the difference in Poisson's ratios remains constant.

2. Elastic module ratios. When $\xi_{2,1} \approx 1$, the relative stresses are of similar size in both layers. By changing this ratio in the layer the material of which is less elastic, the relative stresses are increasing and in the stiffest one they are decreasing.

3. The radial dimensions and cross-sectional area of the layers. As the layer thickness goes smaller, the relative radial stresses become infinitely small, but the hoop stresses is finite, unequal to zero (Bi-axial stress state). The stress state is independent of the dimensions of the bar, where the layer proportions remain constant, i.e. when the scale changes.

4. Material arrangement in the construction. In many cases, the PC-type bar relative stresses are higher than those of the same size NC. Until the PC ratio of elastic modules $\xi_{2,1} >> 1$, or $\xi_{2,1} << 1$ the maximum relative stresses are always obtained in the same material, regardless of the layout of the construction materials.

It was identified that the inner radius $r = 0.5$ m, the outer one $R = 0.745$ m, Poisson's ratios 0.4 and 0.3, the maximum relative stresses reach 15% and while reducing the radius of the inner layer and increasing the thickness of the layers, the relative stress may increase to over 28%.

References

1. **Majzoobi, G.H., Ghomi, A.** Optimisation of compound pressure cylinders.-J. of Achievements in Materials and Manufacturing Engineering, 2006, v.15, Issue.1-2, p.135-145.

2. **Ivanov, S.G., Strikovskii, L.L., Gulyaeva, M.A., Zuiko, V.Yu.** Modeling the mechanical behavior of metal-reinforced thermoplastic pipes under internal pressure. -Mechanics of Composite Materials, 2005, v.41, No.1, p.57-70.

3. **Benz, R., Chikh, N.E., Mesbah, H.** Behaviour of square concrete column confined with GRFP composite wrap. -J. of Civil Engineering and Management, 2008, 14(2), p.115-120.

4. **Hocine, A., Bezazi, A., Boubakar, L., Benamar, A., Kondratas, A.** Multilayer tubular composite reinforced by a liner: Behaviour under pressure loading simulation. -Mechanika. -Kaunas: Technologija, 2005, Nr.5(55), p.11-19.

5. **Tamuzs, V., Tepfers, R., Zile, E., Ladnova, O.** Behavior of concrete cylinders confined by a carbon composite. -Mechanics of Composite Materials, 2006, v.42, No.4, p.433-448.

6. **Tamuzs, V., Tepfers, R., Zile, E., Valdmanis, V.** Stability of round concrete columns confined by composite wrappings. -Mechanics of Composite Materials, 2007, v.43, No.5, p.657-666.

7. **Židonis, I.** Alternative method for the calculation of stress-strain state parameters in normal sections of structural members. -Mechanika. -Kaunas: Technologija, 2007, Nr.5(67), p.24-32.

8. **Bareišis, J., Daniškevičiūtė A., Kleiza, V.** Stress distribution in multilayer structural element subjected to skew bending. Mechanika. -Kaunas: Technologija, 2007, Nr.6(68), p.14-18.

9. **Kuranovas, A., Kvedaras, A.K.** Behaviour of hollow concrete-filled steel tubular composite elements. -J. of Civil Engineering and Management, 2007, v.XIII, No2, p.131-

141.

10. **Kudzys, A., Kvedaras, A.K.** Research on structural resistance and safety of tubular composite members. -Mechanika. -Kaunas: Technologija, 2006, Nr.5(61), p.5-10.
11. **Bareišis, J.** Design and stress state of tensions in multilayer bars, -J. of Composite Material, 2004, v.38, No.5, p.389-393.
12. **Partaukas, N., Bareišis, J.** Revised calculation of strength of a two layer bar under axial loading.-J. of Young Scientists, 2007, No.2(13), p.113-118 (in Lithuanian).
13. **Garuckas, D., Bareišis, J.** The influence of different factors on stiffness and strength of multilayer composite elements.-Mechanics of Composite Materials. -New York: Kluwer Academic/Plenum Publishers, 2003, v.39, No.2, p.153-164.

N. Partaukas, J. Bareišis

DVISLUOKSNIŲ TUŠČIAVIDURIŲ CILINDRINIŲ STRYPŲ ĮTEMPIŲ BŪVIS

R e z i u m ė

Darbe nagrinėjamas dvisluoksnių, tuščiavidurių strypų, veikiamų ašinės apkrovos, įtempių būvis. Sluoksnių medžiaga yra izotropinė, homogeninė, tiesiškai tampri, o sluoksniai koncentriniai cilindrai.

Pateiktas matematinis modelis dvisluoksnio tempiamo ir gniuždomo cilindrinio strypo ašiniams, radialiniams ir žiediniams įtempiams ir jų ribinėms vertėms sluoksniuose nustatyti. Įtempių būviui sluoksniuose įvertinti gautos santykinių įtempių kontakto zonoje išraiškos, kurios įgalina nustatyti, kiek nagrinėjamai konstrukcijai įtempių būvis yra erdvinis, plokščias ar vienašis. Santykinių įtempių rėžiams nustatyti pasiūlytos ribinių verčių kreivės ir pateiktos jų lygtys.

Nustatyta, kad santykiniai įtempiai priklauso nuo Puasono koeficientų verčių, tamprumo modulių bei strypo radialinių matmenų ir sluoksnių skerspjūvio plotų santykių, taip pat ir medžiagų išdėstymo konstrukcijoje. Gautų lygčių analizė parodė, kad tam tikrais atvejais radialiniai ir žiediniai įtempiai gali sudaryti nemažą ašinių įtempių vertės dalį. Maksimalioms santykinių įtempių vertėms nustatyti pasiūlytos ribinių kreivių lygtys.

N. Partaukas, J. Bareišis

THE STRESS STATE IN TWO-LAYER HOLLOW CYLINDRICAL BARS

S u m m a r y

The stress state of two-layer hollow bars in which they are exposed to axial load is analyzed. The layers are made of isotropic, homogeneous, linearly elastic material, and the layers are as concentric cylinders.

A mathematical model for two-layer tension- compression cylindrical bar axial, radial and ring stress and to set the limit values in the layers is presented. To asses the stress condition in the layers the expression of reletive stresses in the contact zone is obtained. It enables to determine how much for the construction under discussion, the stress state is three-dimensional, two-dimensional or axial. For the relative stress determination a limit curve and its equation are proposed.

It has been determined that the relative stresses depend on the values of Poisson's ratio, modulus of elasticity, the radial dimensions and cross-sectional layer areas ratios, also the layout and construction materials. The analysis of the derived equations demonstrated that in certain cases, radial and circular stresses may form a significant part of axial stress value. The maximum relative stress-establish the proposed limit curves equation.

Н. Партаукас, И. Бареишис

НАПРЯЖЕННОЕ СОСТОЯНИЕ В ДВУХСЛОЙННЫХ ПОЛЫХ ЦИЛИНДРИЧЕСКИХ СТЕРЖНЯХ

Р е з ю м е

В работе исследовано напряженное состояние двухслойных полых цилиндрических стержней, нагруженных осевой силой. Слои концентрических цилиндров изготовлены из изотропного, гомогенного, линейно упругого материала.

Представлена математическая модель для определения осевых, радиальных и кольцевых напряжений и их предельных значений в слоях двухслойных стержней при их растяжении и сжатии. Для оценки напряженного состояния в слоях, получены выражения относительных напряжений в зоне контакта, которые позволяют оценить насколько для данной конструкции, напряженное состояние является трехмерным, двумерным или осевым. Для определения предельных значений относительных напряжений установлены кривые предельных значений и предложены их уравнения.

Установлено, что относительные напряжения зависят от значений коэффициента Пуассона, модулей упругости, а также и от отношения радиальных размеров стержня с площадью поперечных сечений слоев и от расположения материалов в конструкции. Анализ полученных уравнений показал, что в определенных случаях, радиальные и кольцевые напряжения могут составить существенную часть осевых напряжений. Для определения максимальных значений относительных напряжений предложены уравнения предельных кривых.